Kernels of Motor Memory Formation: Temporal Generalization in Bimanual Adaptation

Ian S. Howard[1*], Sae Franklin[2] and David W. Franklin[2,3,4*]

[1] School of Engineering, Computing and Mathematics, University of Plymouth, Plymouth, United Kingdom.
[2] Neuromuscular Diagnostics, Department Health and Sport Sciences, TUM School of Medicine and Health, Technical University of Munich, Germany.
[3] Munich Institute of Robotics and Machine Intelligence (MIRMI), Technical University of Munich, Munich, Germany.
[4] Munich Data Science Institute (MDSI), Technical University of Munich, Munich, Germany.

*Correspondence should be addressed to:
ISH: ian.howard@plymouth.ac.uk
DWF: david.franklin@tum.de

Abbreviated title: Temporal Generalization in Bimanual Adaptation

Keywords: motor learning, bimanual context, temporal generalization, dynamic learning, human

Abstract

In daily life, we coordinate simultaneous and sequential bimanual movements to manipulate objects. Despite the complexity, people adapt rapidly, suggesting neural mechanisms optimized for efficient adaptation. Here we extract the temporal kernel that underlies motor memory formation, by testing the contextual effects of past, simultaneous, and future contralateral arm movements and measuring their temporal generalization in three novel bimanual interference tasks. The actions of one arm can serve as a contextual cue for the other arm for all three timing contexts, facilitating dual adaptation. More importantly, the timing of the learned contextual action plays a pivotal role in the temporal generalization. While motor memories trained with past contextual movements generalize broadly, motor memories trained with future movements exhibit limited generalization, and motor memories trained with simultaneous movements do not generalize to past or future timings. This highlights temporal tuning in sensorimotor plasticity: different training conditions yield substantially different temporal generalization.

Introduction

Many everyday tasks require coordinated actions of our two arms. While some tasks, such as opening a jar, require the simultaneous control of both arms, others, such as juggling, involve an initial movement of one hand followed by a subsequent movement of the other hand. Although juggling involves the manipulation of objects that vary in size, weight, or shape, professional jugglers demonstrate impressive hand-eye coordination, producing rapid and accurate object trajectories. Such effective manipulation requires that our sensorimotor system accurately accounts for the dynamics of the objects currently being manipulated, as well as those to be manipulated in the future. Motor learning of such object dynamics during bimanual movement is therefore a fundamental process unpinning human skills.

Adaptation to dynamics occurs through the formation of a motor memory [1–4]. However, these motor memories are not limited to the specific tasks learned, but they generalize to similar movements and tasks, allowing flexible and adaptable motor control [5–8]. As this generalization is thought to stem from learning via neural basis functions, measurement of the extent and type of generalization allows for the investigation of the tuning of these neural basis functions within the sensorimotor control system. While the tuning of these neural basis functions is typically examined as a function of movement direction [6,7,9–11], or kinematics [8,12], the temporal generalization of these learned motor memories has yet to be investigated.

To study the formation, selection and generalization of motor memories, two opposing force fields are often randomly presented during reaching movements. Without any additional cues, this random presentation produces interference: learning each one force field interferes with the memory of the other [13–16]. However, the association of the force field with certain contextual cues allows learning of the

two independent motor memories and appropriate switching of the memories, termed dual adaptation [17–19]. This paradigm allows us to examine which contextual cue types can select and switch between different motor memories within the sensorimotor control system, and identify those cues that do not have such functions [20,21]. Here we use this powerful tool to examine how different temporal relationships between motion of the two hands affect adaptation, specifically focusing on past, simultaneous, and future motions. In unimanual tasks, both past lead-in movements and future follow-through movements allow dual adaptation [19,22,23]. While in bimanual tasks, simultaneous [17,24] and past [25] movements support dual adaptation, little is known about the role of future contextual movements. Moreover, we have no measure of the temporal generalization of these motor memories: how learning at one timing relation transfers to other timing relations. Here, we first investigate how past, simultaneous and future contextual movements of the contralateral hand affect learning opposing force fields. For each trained timing relationship, we then examine the recall of this learned motor memory to range of different temporal relations, enabling us to map out the temporal generalization of these motor memories across different temporal relations, and extract the temporal kernels of motor memory formation.

Results

Three groups of participants performed separate experiments, with each group experiencing a different timing relationship in bimanual training while adapting to two opposing force fields (Fig 1B,C). Each group tested whether past, simultaneous, or future contralateral arm movements can provide a contextual cue for the ipsilateral arm. Here the ipsilateral arm was exposed to opposing viscous curl fields where the direction of the field was determined by the contralateral arm motion. After this adaptation phase, the generalization of the learned motor memory was assessed using probe channel trials (Fig 1D) across various timing intervals between the two arms. These intervals included timings before (past context), during (simultaneous context), and after (future context) the adaptation movement (Fig 1B).

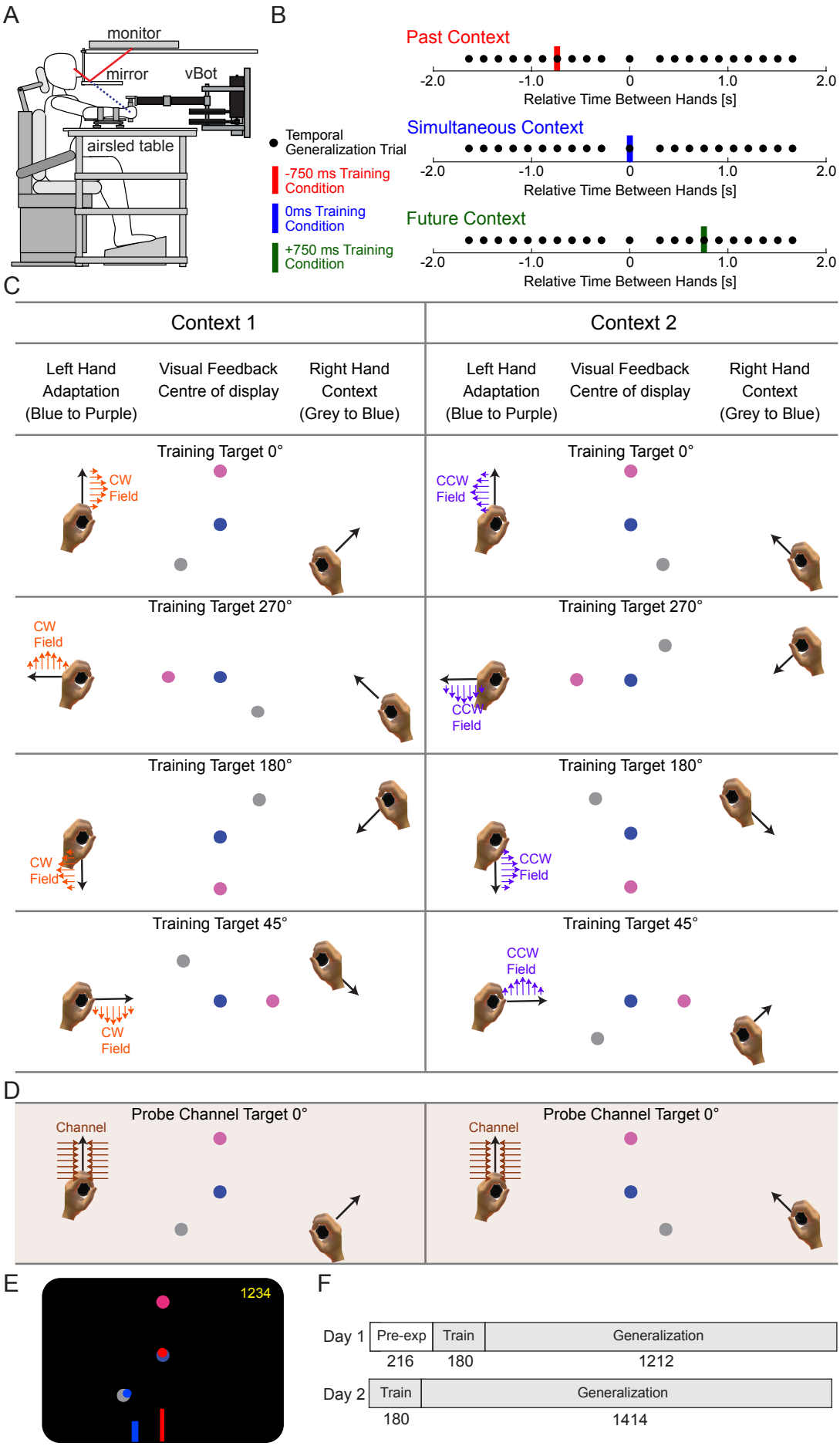
A
monitor
mirror
vBot
airsled table
B
Past Context
Simultaneous Context
Future Context
Temporal Generalization Trial
-750 ms Training Condition
0ms Training Condition
+750 ms Training Condition
-2.0
-1.0
0
1.0
2.0
Relative Time Between Hands [s]
C
Context 1
Context 2
Left Hand Adaptation (Blue to Purple)
Visual Feedback Centre of display
Right Hand Context (Grey to Blue)
Training Target 0°
Training Target 270°
Training Target 180°
Training Target 45°
CW Field
CCW Field
D
Probe Channel Target 0°
Channel
E
1234
F
Day 1
Pre-exp
Train
Generalization
216
180
1212
Day 2
Train
Generalization
180
1414

Figure 1. Experimental Setup and Design. **A.** Experiments were conducted using a bimanual vBOT setup in a virtual reality environment. The participant sits while grasping both handles of the vBOT manipulandum and receiving visual feedback in the plane of movement. **B.** Bimanual Movement Timing Relationships. Three separate experiments were conducted with training at timing relationships of -750 ms (Past Context; red), 0 ms (Simultaneous Context; blue), and +750 ms (Future Context; green). The training time relation between the two hands is shown with the colored bar for each experiment. To test temporal generalization, channel trials were presented at 21 distinct timing relationships, represented by black circles, ranging from -1.8 to +1.8 seconds. Each temporal relationship was tested seven times for each of the two contexts, amounting to a total of 14 tests per relationship. **C.** Experimental protocol for training and testing. The top four rows depict the contextual relationships used in both null and training trials for the four possible adaptation movement directions. The movement of the right-hand provides context, with four distinct starting locations (at 45°, 135°, 225°, and 315°) leading to a central location on the right. The left-hand performs the adaptation movement, executed either in a null field or a viscous curl field. This hand also has four movement directions, beginning from the central position on the left and progressing to specific target locations (0°, 90°, 180°, and 270°). Notably, each adaptation movement direction is paired with two unique contextual movement directions (two columns indicating the two possible contexts). It can be seen that while the two hands were separated by 30 cm, the visual representations of the two hands' movements were aligned such that the end of the movement of the right-hand ended in the center target where the left-hand starts its movement. This involved a visual shift of 15 cm for each hand. **D.** The row (brown shaded region) displays the contextual relationships for channel trials, designed to estimate feedforward adaptation to the viscous curl field. These channel trials proceed solely along the y-axis to an upper target and are linked with two distinct angular contextual movements originating at 135° (right column) and 225° (left column). **E.** Visual feedback provided to the participants. At the bottom of the screen the temporal relation of the right-hand (blue bar) and left-hand (red bar) for the next trial was displayed. The red bar was always in the center of the screen but the blue bar was moved depending on the timing of the relation. Cursors representing the right (blue) and left (red) hands were shown, along with the start and end targets for both movements. The red cursor was moved to the red target while the blue cursor was moved to the blue target. A score representing the number of successful targets was presented at the top right of the screen. **F.** The experimental trial schedule was identical across all three experiments, but each experiment used different training timing relationships. Day 1 started with pre-exposure (Pre-exp) in the null field trials which included testing probe channel trials. The white color indicates that all non-channel trials were performed in a null field to familiarize participants with the manipulanda and the testing procedures. The curl force fields (grey shaded region) were introduced in the Train session (180 trials), followed by a Generalization phase (1212 trials) that provided practice to the bimanual movement relations. Day 2 started with further training (Train), followed by a final Generalization session to study generalization.

The generalization was examined across the three conditions and the different timings using a repeated measures ANOVA finding a significant main effect of timing (Greenhouse-Geisser corrected: $F_{3.204,67.279}=5.863$; $p=0.001$; $\omega^2=0.131$), between subjects effect of experiment condition ($F_{,2,21}=12.493$; $p<0.001$; $\omega^2=0.258$), and interaction between timing and experimental condition (Greenhouse-Geisser corrected: $F_{6.407,67.279}=23.296$; $p<0.001$; $\omega^2=0.544$). Post-hoc comparisons (Holm-Bonferroni corrected) of the interaction effects were performed and reported in subsequent sections.

Experiment 1: Past Context

Experiment 1 (past context) tested the training condition of -750 ms, in which the left-hand adaptation movements were performed 750 ms after a preceding right-hand

contextual movement. That is, the movement of the right-hand acts similar to a lead-in movement prior to the adaptation movement of the left-hand. Before the introduction of the force field, participants made straight movements to each of the four targets with their left-hand (Fig 2A). Once the force field was introduced, participants' movements were strongly curved away from the straight line, with the disturbance direction depending on the sign of the force field (Fig 2B). However, by the end of the exposure phase the movements were disturbed less laterally, and participants made straighter movements to the targets for both force field directions suggesting adaptation to the dynamics (Fig 2C).

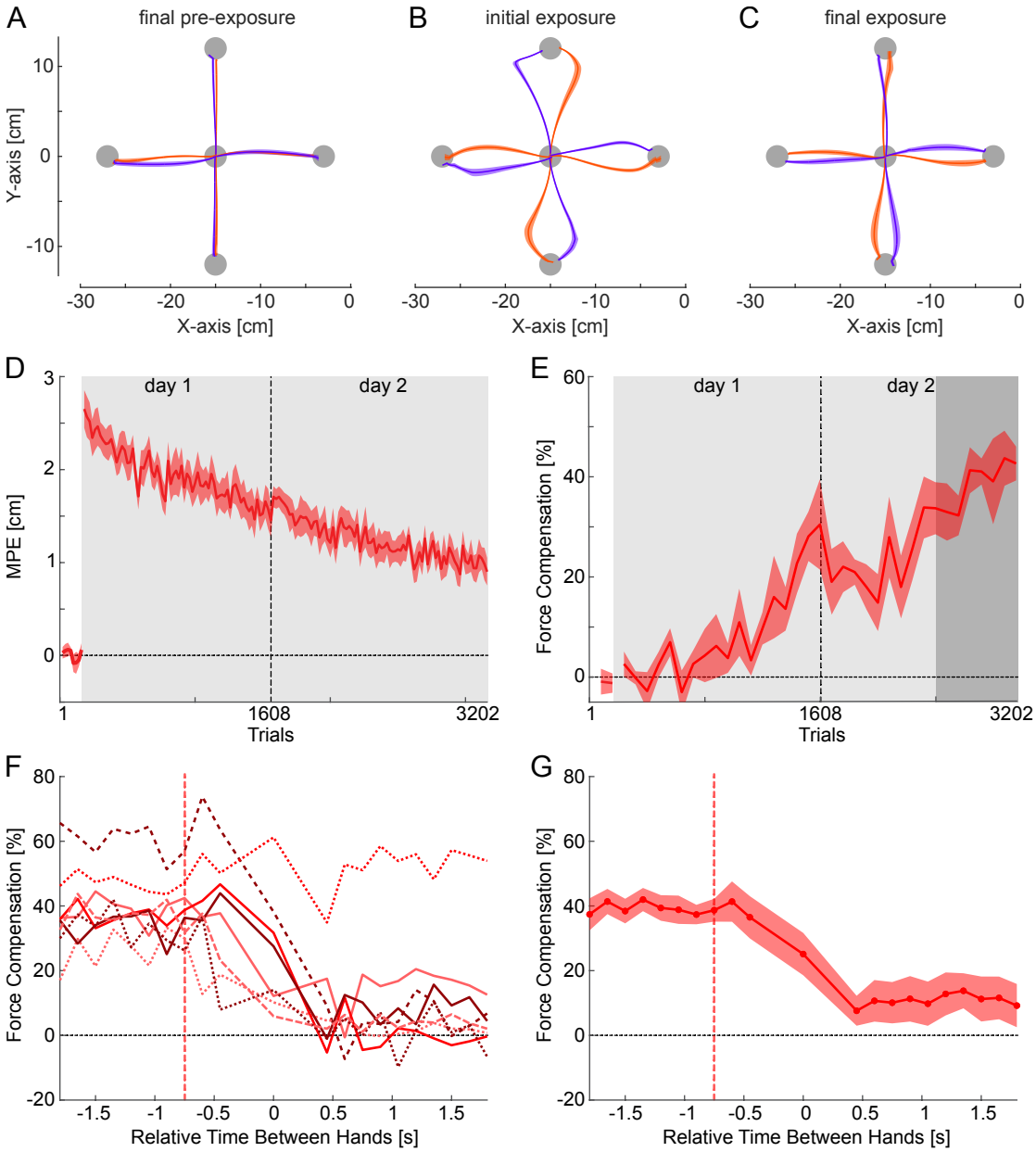

Figure 2: Results for Experiment 1 where the right-hand contextual movement preceded the left-hand training movement by 750 ms (-750 ms condition). **A.** Hand paths in the last block of pre-exposure in the null field condition. The mean and standard error (shaded region) of left-hand paths across participants from the central location to the target are shown for both contextual cue movement

directions. Movements that will be associated with the CW curl force field are shown in orange whereas movements that will be associated with the CCW force field are shown in purple. Within the selected block, the last 8 unique movement directions per participant were used for the calculation. **B.** The hand paths on initial exposure to the curl field. **C.** The hand paths in the final block of curl field exposure. **D.** The kinematic error, measured as maximum perpendicular error (MPE) for the left-hand, plotted over the course of the experiment. The mean (line) and standard error (shaded area) are calculated across the participants. The grey shaded region indicates the period where the force field is applied to the left-hand during the adaptation movements. **E.** Force compensation, expressed as a percentage of complete adaptation to the force field, over the course of the experiment. Grey region indicates the application of the force field, and the dark grey region indicates the period over which the generalization to different timing relations between the two hands was measured. **F.** The temporal generalization of the learned motor memory to all timing relations between the two hands shown for individual participants. Each line denotes a different participant, and the red dashed vertical line indicates the trained relation. **G.** The mean and standard error of the temporal generalization of the learned motor memory across participants. Red circles denote the center of the window over which values were averaged. We see that training at -750 ms led to effective generalization to past contextual movement timing relationships, but not to future contextual movements.

To quantify adaptation, we examined two measures: maximum perpendicular error (MPE) and force compensation. A repeated measures ANOVA indicated that MPE showed strong variations between the pre-exposure, initial exposure and final exposure phases ($F_{2,14}$=129.514; $p<0.001$; ω^2=0.864), which were further tested with post-hoc comparisons. MPE (Fig 2D) was close to zero in the pre-exposure phase, but increased immediately upon the introduction of the force field ($p<0.001$). MPE then reduced over the course of the experiment, with final levels smaller than during initial exposure ($p<0.001$) but not as low as in pre-exposure ($p<0.001$). Force compensation, as measured in channel trials for the training timing relation, was close to zero in the pre-exposure phase. However, force compensation increased slowly during the exposure phase, reaching around 40% by the end of the second day (Fig 2E). A repeated measures ANOVA indicated a strong increase in force compensation between final pre-exposure and final exposure levels ($F_{1,7}$=188.732; $p<0.001$; ω^2=0.887).

The temporal generalization of the learned motor memory was examined towards the end of the exposure phase by introducing probe channel trials. In these trials, the timing between the right contextual hand movement and the left-hand adaptation movement was changed from -750 ms to one of 21 values between -1.8 and +1.8 seconds (Fig 1B). The force compensation observed in these trials enabled us to assess the extent to which the learned motor memory was specific to the trained condition, or whether it generalized to other timing relations. These timing relations included both those matching the trained relation between the hands (past contextual movements) and extended to those that did not (synchronous or future contextual movements).

The temporal generalization of the motor memory after training at -750 ms demonstrates consistent and effective generalization to other past contextual movements (Fig 2G), with all timing relations between -1.8 and -0.45 s exhibiting

around 40% compensation. However, there was little transfer to future movements (approximately 10%). Post-hoc comparisons supported these findings with no significant differences across any past movement timings (all $p=1.0$) but strong differences between all past movements and all future movements (all $p<0.001$), and no significant differences between all past movement timings (all $p=1.0$). While the simultaneous condition was different than the nearest future condition ($p=0.041$), there were no significant differences with any of the other past (all $p>0.078$) or future conditions (all $p>0.188$). This generalization pattern was consistent across all but one participant, who showed flat generalization across all training relations (Fig 2F). Overall, we find that the past contextual bimanual movement generalizes strongly to all other past contextual movement timings and partially to the synchronous condition. However, there is little or no generalization to the future contextual conditions.

Experiment 2: Simultaneous Context

In the second experiment (simultaneous context), the onset of both the adaptation and contextual movements occurred simultaneously (0 ms). In the pre-exposure phase, participants made straight movements towards each of the four targets with their left-hand (Fig 3A). Again, once the force field was introduced, participants' movements were strongly disturbed in the direction of the applied force field (Fig 3B). However, by the end of the exposure phase, the participants made straight movements to the targets for both force field directions (Fig 3C). The kinematic error (MPE) increased immediately upon introduction of the force field (Fig 3D), but reduced over the course of force field exposure. A repeated measures ANOVA found significant differences across the phases of the experiments ($F_{2,14}=105.044$; $p<0.001$; $\omega^2=0.886$), with initial exposure larger than pre-exposure ($p<0.001$) and final exposure ($p<0.001$), but no difference between pre-exposure and final exposure ($p=0.097$). Force compensation steadily increased throughout the exposure phase, reaching approximately 50% by the end of the second day (Fig 3E). A repeated measures ANOVA found a strong increase in force compensation between final pre-exposure and final exposure levels ($F_{1,7}=117.522$; $p<0.001$; $\omega^2=0.867$). Thus, participants were able to adapt to the two opposing force fields with simultaneous contextual movements of the other hand.

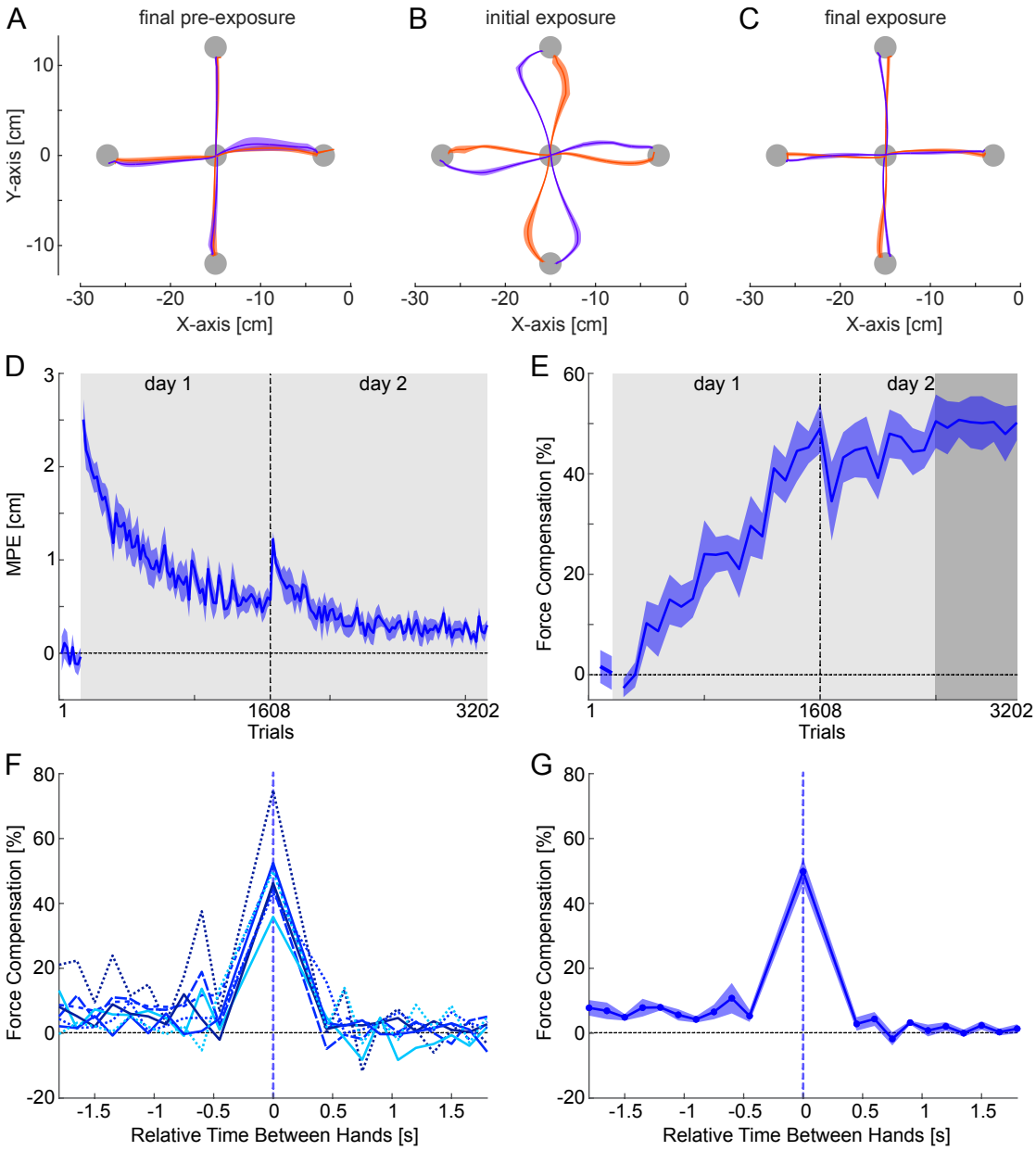

Figure 3: Results for Experiment 2 using training at a 0 ms synchronous context timing relationship **A.** Hand paths in the last block of pre-exposure in the null field condition are shown for both contextual cues. **B.** The hand paths on initial exposure to the curl field. **C.** The hand paths in the final block of curl field exposure. **D.** The kinematic error, measured as maximum perpendicular error (MPE) for the left-hand, plotted over the experiment. **E.** Force compensation, expressed as a percentage of complete adaptation to the force field, over the experiment. Grey region indicates the application of the force field, and the dark grey region indicates the period over which the generalization to different timing relations between the two hands was measured. **F.** The temporal generalization of the learned motor memory to all timing relations between the two hands, shown for individual participants. Each line denotes a different participant and the blue dashed vertical line indicates the trained relation. **G.** The mean and standard error of the temporal generalization of the learned motor memory across participants. Training at 0 ms leads to limited generalization to past or future contextual movement timing relationships.

The temporal generalization of the learned motor memory was again examined at the end of the second day of the experiment, using probe trials at different contextual timing relations ranging between -1.8 and +1.8 s. The temporal generalization of the motor memory after training at 0 ms had a very strong decline in compensation when the onset of the contextual movement was either advanced or delayed (Fig 3G). Post-hoc comparisons supported the strong decreased away from the trained condition. The simultaneous timing was significantly different than all past (all $p<0.001$) and all future (all $p<0.001$) timings, but there were no significant differences between any of the past and future timings (all $p=1.0$). This generalization pattern was consistently expressed by all participants (Fig 3F). Overall, we find that while strong learning occurs in the 0 ms condition (50%), there is limited transfer to past contextual movements (<10%), and no transfer to future contextual movements (0%).

Experiment 3: Future Context

In the third experiment (future context), left-hand adaptation movements were conducted prior to right-hand contextual future movements (+750 ms), such that the right-hand contextual movements acted as a planned future contextual cue. During the pre-exposure phase, participants made straight reaching movements (Fig 4A), which were strongly disturbed in the initial exposure of the force field (Fig 4B). However, by the end of the exposure phase the participants made fairly straight movements to the targets (Fig 4C) indicating that some compensation to the applied dynamics was achieved. Again, the kinematic error (MPE) increased immediately upon introduction of the force field (Fig 4D), but reduced over the course of force field exposure. A repeated measures ANOVA found significant differences across the phases of the experiments ($F_{2,14}=228.999$; $p<0.001$; $\omega^2=0.944$), with initial exposure larger than pre-exposure ($p<0.001$) and final exposure ($p<0.001$), although final exposure was still higher than pre-exposure ($p<0.001$). Force compensation increased throughout the exposure phase, reaching approximately 40% by the end of the second day (Fig 4E). A repeated measures ANOVA found a strong increase in force compensation between final pre-exposure and final exposure levels ($F_{1,7}=67.810$; $p<0.001$; $\omega^2=0.818$).

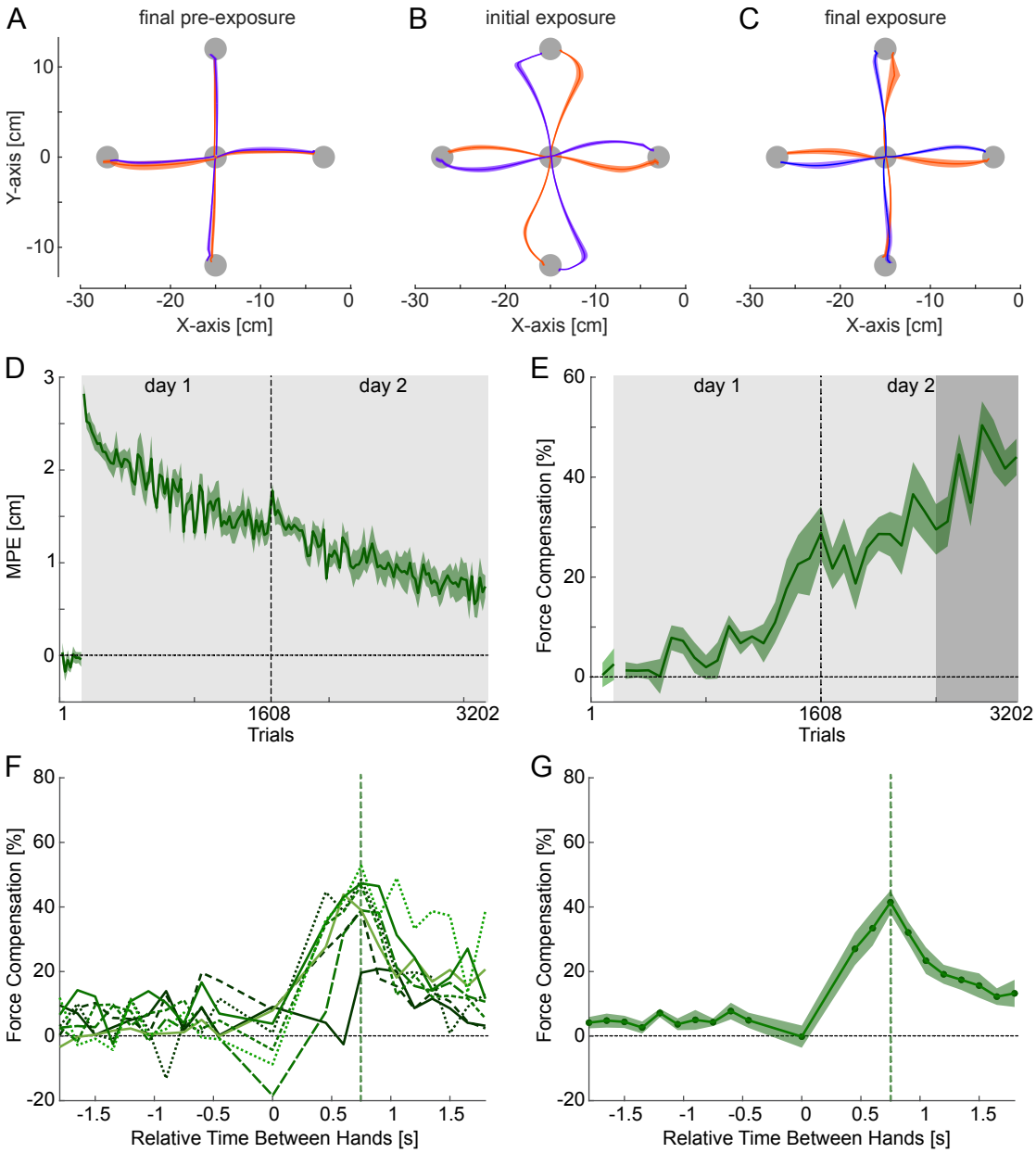

Figure 4: Results for Experiment 3 where the right-hand contextual movement followed the left-hand training movement by 750 ms (+750 ms condition). **A.** Hand paths in the last block of pre-exposure in the null field condition. **B.** The hand paths on initial exposure to the curl field. **C.** The hand paths in the final block of curl field exposure. **D.** The kinematic error (MPE) for the left-hand. **E.** Force compensation, expressed as a percentage of complete adaptation to the force field. **F.** The temporal generalization of the learned motor memory to all timing relations between the two hands shown for individual participants. Each line denotes a different participant and the green dashed vertical line shows the trained relation. **G.** The mean and standard error of the temporal generalization of the learned motor memory across participants. Training at +750ms leads to a swift decline in generalization to other future contextual movement temporal relationships, with no generalization to past contextual movements.

The temporal generalization of the learned motor memory was once again examined at the end of the second day of the experiment, using probe trials at different contextual timing relations ranging between -1.8 and +1.8 s. The temporal generalization of the motor memory after training at +750 ms shows a marked

decrease in compensation when the onset of the contextual movement deviated from the trained timing relation (Fig 4G). The trained timing (0.75 s) force compensation generalizes well to nearby timings (0.45 s, 0.6 s, 0.9 s), with no significant differences between any of the three conditions (all $p>0.685$). However, the force decreases away strongly from the three times with the strongest responses (0.6 s, 0.75 s, and 0.9 s) to the 0 ms timing (all $p<0.001$), all past timings (all $p<0.001$), and all future timings greater or equal to 1.6 s (all $p<0.01$). The decay to longer future times already decreased from the peak compensation by the 1.05 s timing ($p=0.022$). However no significant differences were found between any of the past, simultaneous, or future timings larger than 1.35 s (all $p>0.491$). This generalization pattern was consistent across all participants (Fig 4F). Overall, we observed a significant decrease in compensation when the onset of the contextual movement was either advanced or delayed relative to the training time, even for other future contextual timing relations. There was no transfer to the synchronous timing relation or to past movements.

Comparison Across Experiments

The three experiments followed identical designs, except for the timing relation between the two arms in the training condition, allowing for comparison across experiments. At the end of the force field exposure (final block of day 2), the simultaneous 0ms condition (Experiment 2, blue) yielded the straightest left-hand trajectories (Fig 3B), whereas both the past (Experiment 1, red) and future (Experiment 3, green) contexts remained slightly more curved (Figs. 2B, 4B). These trends align with the final levels of MPE values observed at the end of the experiments (Fig 5A, B). The simultaneous context (blue) exhibited the most rapid decrease in MPE, whereas the future context (green) and past contexts (red) had slower reductions in MPE. However, all three experiments showed clear reductions in MPE over the course of the experiment. An ANOVA comparing the final levels of MPE in the last block of the experiment found significant differences between the experiments ($F_{2,21}=7.503$; $p=0.003$; $\omega^2=0.028$), with the simultaneous context showing a lower final MPE than either the past ($p=0.004$) or future ($p=0.023$) contexts, but no significant differences between the past and future contexts ($p=0.341$).

Force compensation exhibited similar patterns across all three experiments (Fig 5C). The simultaneous context (blue) showed the fastest increase in adaptation, with little differences in the development of the force compensation between the past (red) and future (green) contexts. However, all three experiments achieved comparable final compensation levels at the end of the experiment (Fig 5D), with no significant differences across the three conditions ($F_{2,21}=1.350$; $p=0.281$; $\omega^2=0.351$). Overall, the results indicate that the timing relationships in all three contextual timing relationships act as effective cues for learning and adapting to opposing dynamics in the contralateral arm, facilitating the adaptation to opposing force fields.

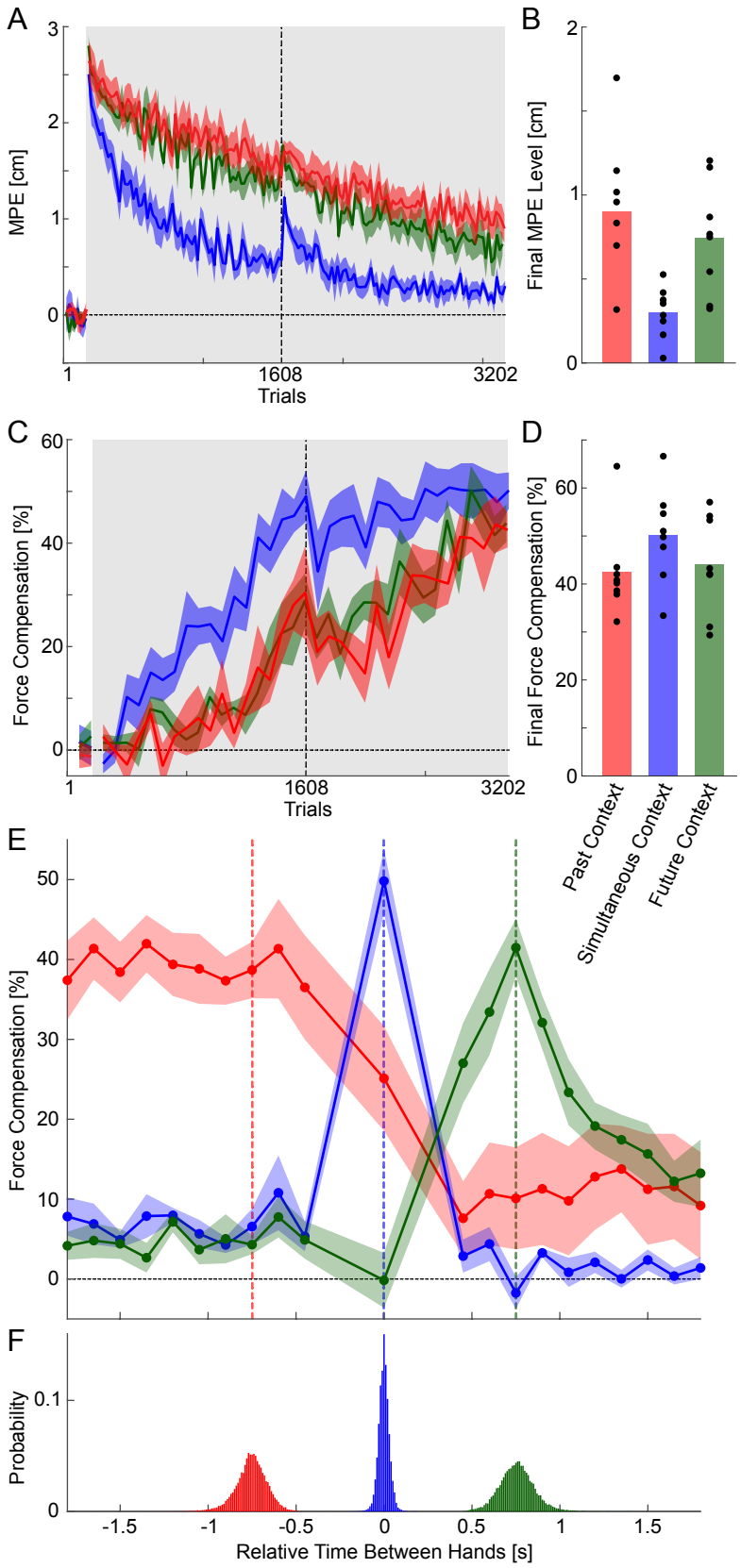

Figure 5. Comparison across the three experiments where participants were trained with either past (-750 ms; red), synchronous (0 ms; blue) or future (+750 ms; green) timing relation. **A.** Comparison of kinematic error (MPE) changes across the experiment. **B.** Final levels of MPE at the end of the experiment. Colored bars indicate the mean MPE across participants in the final exposure block, while black circles represent individual participant values. **C.** Force compensation evolution across the three

experiments. **D.** Final force compensation values across the three experiments (mean and individual participants) are shown for the final exposure block. **E.** Comparison of temporal generalization across bimanual timing relations after training at one of the three timing relations. Colored vertical lines illustrate the trained relation for each experiment. Solid lines depict the mean, and shared regions the standard error of the mean, across participants. Dot placements on the plot indicate the central location and the estimated mean compensation value for each bin. **F.** Histograms present relative movement initiation offsets between the two arms for all null practice and curl field training trials across the three experiments. Results for the -750 ms past movement context experiment are in red, the synchronous 0 ms movement context experiment in blue, and the +750 ms future movement context experiment in green.

A comparison of the temporal generalization across the three experiments reveals the distinct effects resulting from training at the three distinct timing relations (Fig 5E). The synchronous context (blue) has the highest peak of adaptation at the training condition with negligible generalization to either past or future timing relations. In contrast, both the past (red) and future (green) timing training contexts demonstrate generalization across various timing relations. However, the future context (green) shows selective generalization within different future timings (decreasing away from the training condition), and no transfer to the synchronous or past timings. Conversely, the past context (red) exhibits strong generalization across all past timing relations, partial transfer to the synchronous condition, and limited transfer (10%) to future conditions. Post-hoc comparisons showed strong differences between the three experimental conditions, with the past context (red) exhibiting significant differences (all $p<0.001$) to both the simultaneous and future contexts at every past timing (-1.8 s to -0.45 s). All three contexts were significantly different from one another at the simultaneous 0.0 s timing (all $p<0.03$). Similarly, the future context was different from both other contexts at the trained 0.7 s timing (all $p<0.001$). The future context (green) was also significantly different from the simultaneous context (blue) over all tested timings between 0 s and 0.9 s (all $p<0.043$). However, there were no significant differences between any of the three contexts in the timings from 1.06 to 1.8 s (all $p>0.123$). Overall, we find distinct temporal generalization across the three experiments.

We propose that the variations in the temporal generalization patterns across the three experiments are indicative of different tuning functions within the sensorimotor control system for contextual movements. These variations may play a key role in the learning of coordinated actions across limbs. However, an alternative explanation could be different levels of variability in the training times, which might directly contribute to these patterns. To explore this possibility, we quantified the variability in training timing for each experiment (Fig. 5F). Here each histogram represents the distribution of the relative start times between the arms during the training movements for each experiment. The synchronous context (blue) had the narrowest spread of timings in the training condition, with times very close to the requested 0 ms separation. In contrast, the training conditions for the past (red) and future (blue) contexts exhibited slightly greater variability in onset times. However, this variability was significantly smaller than the width of the generalization tuning functions observed, particularly in the case of the past and future contexts. This implies that the

observed generalization is more likely to reflect underlying neural circuitry rather than being merely a result of variations in the training conditions.

Discussion

In this study, we explored the intricate relationship between right arm contextual movements and motor learning and recall in the left arm using a force field interference task. In three experiments, participants learned to compensate for two opposing force fields. The directions of these force fields were uniquely associated with the relative angle of movement of the right arm compared to the left arm. Each experiment trained participants at a distinct timing of the relation between the right- and left-hand movements (past context, simultaneous context or future context) and assessed temporal generalization over a wide range of past, simultaneous and future timings. Participants in all three experiments successfully learned to predictively adapt to the two opposing force fields, achieving 40-50% final adaptation. Our evaluation of how this learned motor memory generalized across different movement onset timings yielded three key findings. First, training in the simultaneous context led to recall primarily only at the learned timing, with a marked steep decrease in transfer to other timings. Second, training with past movements resulted in broad generalization to other past timings and, to a lesser extent, to simultaneous movements, but showed minimal transfer to future contextual movements. Lastly, training in future contexts led to generalization to close-by future timings, but this effect diminished for timings far removed from the training context, with no significant observable transfer to simultaneous or past contexts. Overall, our data highlights the diverse patterns of temporal generalization based on the timing relationships of the training, illuminating the distinct characteristics and implications of past, simultaneous, and future contexts in bimanual dual adaptation tasks.

All three experiments confirm that bimanual motion serves as a strong contextual cue for learning opposing dynamics. Specifically, the relative motion of one limb can predictively influence the control of forces in the other limb, regardless of whether this contextual movement occurs before, simultaneously with, or after the adaptation movement. This finding aligns with previous research, which has shown that simultaneous movements of one arm can reduce interference during learning in the other arm [17,24,26]. For instance, the ability to switch between two motor memories is facilitated when one hand is either moving or stationary [17]. Similarly, significant effects have been observed when the contextual arm moves in the same or opposite direction as the adaptation arm [24] and when the relative angle between the two hands varies [26]. In unimanual movements, recent studies have demonstrated that both prior [9,12,19] and future motions [22,23], when closely timed, can facilitate the learning of separate motor memories. The phenomenon that past motion influences learning has also been confirmed in bimanual movements, as evidenced by research showing that prior motion of the left-hand can cue different motor memories in the right-hand [25]. However, the effect of future movements as an effective context had not been established. Our current study builds upon the previous findings by demonstrating that future contextual movements of one arm can also drive the learning of

independent motor memories in the contralateral limb. This mirrors observations in unimanual studies but differs in the level of adaptation; in our study, both past and future contextual movements resulted in similar levels of adaptation, unlike in unimanual studies where adaptation for future ('follow-through') movements was approximately half that for past ('lead-in') movements [19,22,23].

One important difference in our experimental design, compared to these previous studies [17,24–26] is that our participants never received online visual feedback about the movement of their contextual (right) arm, whereas such feedback was consistently presented in the previous research. This is an important control measure, as visual motion of the cursor alone is a strong contextual cue [10,12,19,27]. Thus, the inclusion of visual motion in the bimanual conditions in previous studies might reflect the impact of this visual element rather than the physical motion of the contralateral limb. Although Gippert and colleagues [25] included a visual 'bimanual' condition showing little adaptation, the visual cursor movement was offset 10 cm from the adaptation movement. This offset might have diminished the contextual strength or functioned similarly to a weaker peripheral visual cue [20]. In our study, we demonstrate that past, simultaneous and future movement of the contralateral limb, can facilitate the separate learning of motor memories, even in the absence of visual information. This finding supports the interpretations of these previous studies [17,24,26], and highlights the robustness of limb movement as a contextual cue in motor learning.

Our work extends these former studies, by examining whether the learning generalizes across a range of timing relations between the two limbs. Training at one timing relation not only transfers to other timing relations, but this temporal generalization distinctly varies depending on whether the contextual movement occurs before, simultaneously with, or after the adaptation movement. While numerous studies have demonstrated generalization of a learned motor memory across variations in movement directions [6,7,28], kinematics [8,12,29] and postures [1,30,31], this study is the first to show such generalization to different temporal relations. Just as generalization across directions has been used to infer the neural basis functions underlying motor memories [29,32–34], we propose that the pattern of the temporal generalization reflects the temporal tuning of these neural basis functions.

The three experiments exhibit different levels of variability in the timing between limbs during training (Fig 5F). While both the past and future contexts show similar variability in the timings of the two limbs, the simultaneous context has a narrower range of timing variability, indicating a greater consistency in this group. This is unsurprising as simultaneous bimanual movements are generally easier to perform than non-simultaneous movements [35–37]. Kinematic variability of contextual movements (e.g. follow-through) during adaptation reduces the learning rate [22,38]. Therefore, it is plausible that temporal variability of contextual movements had a similar effect, given that we observed slower final adaptation levels for the past and future contexts. However, in the current study it is impossible to separate the effect of temporal variability from that of the training condition. Importantly, the past and future conditions exhibit broader temporal generalization than the simultaneous condition, which shows almost no generalization to other timing relations. Although

the differences in generalization could arise from the restricted exposure to specific timings during training, we believe that this is unlikely. First, despite similar variability in training times, there are strong differences in generalization between past and future contexts. Second, the past context generalizes to simultaneous and, to a lesser degree, future times, suggesting that generalization is not confined to the variability encountered during training. In fact, both past and future contexts show generalization that extends far beyond any variability in training times. Therefore, we propose that the observed differences likely stem from variations in the inherent use of contextual information for generating natural behavior, and therefore in the underlying neural circuitry involved in learning and executing coordinated bimanual movements.

Extensive research has examined behavioral and neural mechanisms underlying bimanual actions [39]. Neural activity associated with generating and controlling bimanual movement involves interactions between both cerebral hemispheres to learn the control [40]. This includes both contralateral and ipsilateral primary motor cortex, where bimanual or unimanual movements exhibit different patterns of neural activity [41–43]. The cerebellum [44–46], parietal, and frontal areas also play significant roles [47]. While we cannot elaborate on the neural regions responsible, our work examines the shape of the neural basis functions that give rise to our motor memories through testing the generalization. It has been suggested that local neural basis functions form the building blocks of motor memories [29,32–34], allowing flexible generalization to similar states. Normally, these basis functions exhibit Gaussian-like tuning. However, our findings reveal that temporal generalization can display significantly different patterns depending on the training conditions, ranging from broad generalization across times in the past context to narrow tuning in the simultaneous context.

Although there is significant interest in understanding the neural mechanisms underlying sensory-motor behavior, additional approaches can provide insights into the operation of the human nervous system from a normative perspective [48–51]. In real-world tasks, prior movements play a crucial role in establishing anticipatory muscle activation patterns [52]. This is especially true for bimanual actions, where coordination between both arms is essential. Here, anticipatory adjustments in both hands are observed, ensuring seamless and synchronized actions [53]. As past actions can lead to future interactions, requiring compensatory forces, not just immediately but across different times, this might explain our finding of strong generalization across all past timings, including simultaneous movements. Adjustments to forces produced by the other limb are particularly relevant (and frequent) in simultaneous movements, where the action of one limb often directly produces forces in the other limb; for example, when opening a jar or pouring a glass of water. Such interactions between limbs are often so closely linked in time that we consider such actions as evidence for predictive models [54–57]. Therefore, we might expect that trained simultaneous interactions show limited generalization to either past or future contexts. While future movements might not typically be considered to generate interaction forces due to the direction of causality, we know that future movements, including follow-throughs, are important aspects of many tasks. A follow-through movement guarantees a smooth termination of the movement and aids in dissipating

energy to reduce injury risk [58]. Extending our previous unimanual studies [22,23], we also show that future movements of the other limb drive adaptation to opposing dynamics. It is important to consider an evolutionary perspective [59,60]. In locomotion on variable ground, movement of one limb requires compensatory motions in the other limb. This occurs both from past movements and in preparation for future movements. That is, preparing for a future step requires adaptations within the current movement. Moreover, the temporal interval between steps can vary widely. This locomotion-based perspective might explain why we find such plastic adaptation and generalization to past and future movements of the opposite limb, whereas the narrow generalization of simultaneous movements might reflect the tight coupling in object manipulation.

Overall, this work highlights the plasticity of the sensorimotor control system, demonstrating that slightly different training conditions produce widely different temporal generalization. These differences might be explained by considering the influence of different tasks on the neural circuitry over evolutionary timescales. While state space model approaches have been used to explain adaptation to multiple dynamics [61,62], more recent work has suggested that contextual inference underlies our ability to adapt to novel dynamics with different contexts [63,64]. Future work will be needed to explore the extension of these models in explaining and predicting the varied patterns of adaptation and generalization induced by different contextual cues in sensorimotor adaptation.

Methods

Experimental Setup

Participants. Twenty-six human participants were randomly allocated to three experiments. Two participants were removed from further analysis as they were unable to learn to predictively compensate the viscous curl field, leaving twenty-four. This resulted in eight participants for each of Experiment 1 (3 females, average age 24.6 ± 2.4 years), Experiment 2 (5 females, average age 28.4 ± 8.5 years), and Experiment 3 (3 females, average age 25.6 ± 2.7 years). All participants were right-handed as determined by the Edinburgh Handedness Questionnaire [65] and naïve to the purposes of the experiment. Prior to the experiment, each participant provided written informed consent. For participants tested in Plymouth (n=3), the experiments were conducted in accordance with ethics approval by the University of Plymouth ethics committee. For participants tested in Munich (n=23), the experiments were conducted in accordance with ethics approval by the Ethics Committee of the Medical faculty of the Technical University of Munich. Each participant completed one experiment, consisting of two experimental sessions over two consecutive days. Each session lasted approximately three hours, resulting in a total duration of approximately six hours for each participant.

Apparatus. Participants performed all experiments using a bimanual vBOT planar robotic manipulandum paired with an associated virtual reality system [66] (Fig. 1a). The positions of the handles were calculated based on measures using optical motor encoders sampled at 1000 Hz, and torque-controlled motors allow the application of end-point forces. A force transducer (Nano 25; ATI), mounted under the left handle, measured the applied forces. These force signals were low-pass filtered at 500 Hz using 4th-order analogue Bessel filters before digitization. To minimize body movement, participants were comfortably seated in a sturdy chair positioned in front of the apparatus and were firmly strapped against the backrest with a four-point seatbelt.

During the experiment, participants held the left and right robot handles with their respective hands, with their forearms supported by air sleds. This setup effectively restricted arm movements to the horizontal plane and provided full support of the mass of their arms during the experiments. Participants could not directly observe their arms or hands; instead, veridical visual feedback was provided using a 2D virtual reality system to overlay images of the left- and right-hand starting and target locations (all with a 1.25 cm radius), as well as hand cursors (a 0.5 cm radius disk). This arrangement ensured that the visual cursor appeared to the participant in the same plane as their hand. Data were sampled at 1000 Hz and archived for offline analysis.

Force Fields. Movements of the right-hand, termed the contextual movement, were always performed in a null field. Movements of the left-hand, termed adaptation movements, were performed in one of three different environments: null field, curl force field, or channel trials. During trials in the null field, no external forces were applied on the hands by the robotic manipulandum. During trials in which a curl force field was present, a velocity-dependent curl force field [67] was implemented as:

$$\begin{bmatrix} F_x \\ F_y \end{bmatrix} = k \begin{bmatrix} 0 & -1 \\ 1 & 0 \end{bmatrix} \begin{bmatrix} \dot{x} \\ \dot{y} \end{bmatrix} \quad (1)$$

The field constant k was set to a value of ±13 $Nm^{-1}s$, where the sign determines the direction of the force field, which was either clockwise (CW) or counter clockwise (CCW). Each participant was exposed to both force field directions, where the direction of the force field was consistently associated with a specific relation to a contextual movement of the participant's right-hand. The relationship between the directions of the contextual movements and the curl field direction (CW/CCW) was counterbalanced across participants. In the channel trials, a mechanical channel [68,69] was implemented with a stiffness of 6,000 Nm^{-1} and a damping of 30 $Nm^{-1}s$. This mechanical channel was applied perpendicular to the direction of motion, extending from the start to the final target. Channel trials were exclusively conducted for movements towards the 0° target.

Experimental Design

To investigate the temporal generalization of contralateral arm movements, we conducted three distinct bimanual interference experiments, each involving a different group of participants. Each experiment trained the participants at a specific timing relation between the two hands and then assessed their ability to generalize this training across a broad range of timing relations (Fig 1B). Almost all aspects of the three experiments were identical with the only differences being the bimanual timing relationship (dwell time) for the training movements, which are the temporal gap between contextual and adaptation movements (Fig 1B, colored bars).

In all experiments, the right-hand movement, defined as the contextual movement, was initiated from a start location towards the center point. Conversely, the left-hand movement, defined as an adaptation movement, began at the center point, and was directed towards a target location. All trials involved 12 cm active movements of both hands. In each experiment, the bimanual timing relation of the training movements was changed (Fig 1B). Experiment 1 (past context) utilized a contextual movement that preceded the adaptation movement. Experiment 2 (simultaneous context) utilized a contextual movement that coincided with the adaptation movement. In Experiment 3 (future context), utilized a contextual movement that followed after the adaptation movement.

The adaptation movement performed by the left-hand was associated with either a clockwise (CW) or counter clockwise (CCW) curl force field during the exposure phase of the experiment. There were four different directions of adaptation movements, oriented at 0°, 90°, 180° and 270°. Each direction of the adaptation movement was associated with two distinct directions of the contextual movement. Specifically, the contextual movements were either rotated 45 degrees clockwise or 45 degrees counter-clockwise, to provide the contextual cue (see Fig 1C). Consequently, this resulted in eight unique combinations of contextual and adaptation movements. For half of the participants, context 1 was associated with the CW curl force field and context 2 was associated with the CCW curl force field. For the remaining participants this association was reversed. Importantly, although the physical locations of the handles were shifted away from the center of the workspace to prevent collisions between the two hands, the visual feedback for the task was centered in the workspace. This positioning meant that the endpoint of the contextual movement coincided with the start of the adaptation movement. All contextual movements performed by the right-hand occurred in null fields. During the exposure phase of the experiments, the adaptation movements of the left-hand were always performed in either a curl force field or within a mechanical channel.

All trials consisted of a two-part movement produced by both hands. Each trial began when the two cursors, representing the two hands, were placed in their respective starting circles. Although participants could not see their arms and hands, the two hand cursors were presented in different colors: red for the left cursor and blue for the right cursor. The starting circle for the right-hand was grey, while that for the left-hand was blue. Participants were instructed to keep their hands in these circles until an auditory cue signaled the initiation of the series of the movements. The order of the hand movements was displayed at the bottom of the screen, with red and blue

bars indicating the timing of each hand's movements on the time scale along the x-axis (Fig. 1E). The timing of the movements for both the right- and left-hands were cued with auditory beeps.

Upon the presentation of each auditory cue, participants were required to move each of their hands (as indicated by the display at the bottom of the screen) to the appropriate target circle and stop there. Once the red cursor (representing the left-hand) was successfully placed into the final target circle, the circle's color changed from pink to red. Similarly, when the blue cursor reached the center target circle, the circle's color changed from light to dark blue. Importantly, visual feedback of the trajectory of the contextual movement was never shown to the participants. Therefore, participants had to rely on this color change (from light to dark blue) to determine whether they had successfully positioned their cursor in the target.

In each experiment, different time intervals were set between the start of the movement for the left- and right-hands: -750 ms, 0 ms, or +750 ms. The trial ended once both hands remained stationary within their respective target locations. At the end of each trial, the robotic manipulandum passively moved the participants' hands to the next starting locations. The next trial commenced once the handles had been stationary within the start location for 300 ms. Participants were required to take short breaks approximately every 200 trials but were also allowed to rest at any time between trials by moving the cursors out of the start targets.

At the end of each trial, participants received feedback. The movement speed of each hand was evaluated based on the peak velocity, and this feedback was provided immediately after every trial. The speed feedback for each hand was displayed at the top left of the screen as two vertical bars, representing individual hands. The appropriate speed range was indicated by two horizontal lines. If the peak speed of a hand's movement fell within the desired range, its corresponding vertical bar was colored green. Conversely, if the movement was too fast or too slow, the bar was colored red.

Participants were encouraged to maintain their movement speed within the specified range (38.25 to 51.75 cm/s), as indicated by the velocity indicator. If a participant's hand moved from the start position before the auditory cue, or if they failed to complete a trial by moving their hands to the targets within the maximum time limit (5 seconds), the trial was cancelled. A trial was also cancelled if the time difference between initiating the movements of both arms exceeded a certain threshold value. This threshold was set at 200 ms for simultaneous context experiments and at 950 ms for the past and future context experiments. Cancelled trials were added to the end of each block to be repeated. A trial was considered successful when the movement speed of both hands fell within the specified range. For each successful trial, one point was added to the participant's score, displayed at the top right of the screen.

Probe Channel Trials.

To estimate both the predictive compensation for the force field as part of the adaptation process, and to measure the temporal generalization over a range of

timing relations between the two limbs, we introduced probe channel trials. Throughout the experiment, on randomly selected trials, channel trials matching the training condition were introduced to estimate the feedforward adaptation to the curl force field. These channel trials were exclusively introduced for the adaptation movements (left-hand) moving directly forward to the final target, and were associated with two possible angular contextual movements (as shown in Fig 1D). Furthermore, to examine the generalization of learning related to contextual movements made at specific temporal training relationships, we assessed the recall of adaptation across a range of timing relationships from ±1.8 seconds. Specifically, channel trials were conducted at 21 different requested bimanual timing relationships: [-1.8, -1.65, -1.5, -1.35, -1.2, -1.05, -0.9, -0.75, -0.6, -0.45, 0, 0.45, 0.6, 0.75, 0.9, 1.05, 1.2, 1.35, 1.5, 1.65, 1.8] seconds. The bimanual timing relationships used in the three experiments, as well as those used to probe generalization, are illustrated in Fig. 1B (black dots). All probe channel trials were limited to the forward reaching movements (target 0°) only.

Protocol

Participants performed two experimental sessions, which were always conducted on two consecutive days. On day 1, participants completed 1608 trials, and on day 2, they completed 1594 trials, totaling 3202 trials for the full experiment (Fig 1F).

Day1. The first session consisted of a pre-exposure phase in the null field, an initial force field exposure in the training phase, and then continued force field exposure in the generalization phase. Temporal generalization probe trials were introduced during both the pre-exposure and generalization phases in order to familiarize participants with executing movements of the two arms at different timing relations.

Pre-exposure phase: Participants began with 36 trials in the null field, divided into two blocks of 18 trials each. Each block consisted of sixteen null field trials (two for every movement type) and two channel trials (one for each context). This was followed by two blocks of mixed null field and generalization trials, totaling 180 trials. Each of these blocks comprised 48 null field trials and 42 generalization channel probe trials. These probe trials were designed to examine the recall of compensation for adaptation across all 21 different timing relationships, spanning the ±1.8 second range for both contexts. The total length of the pre-exposure phase was 216 trials.

Training phase: Participants were then exposed to ten blocks of trials, where each curl force field was associated with one of the two contextual cues. Each block, consisting of 18 trials, included 16 curl field trials (two for every movement) and 2 channel trials (one for each context). This phase totaled 180 trials.

Generalization phase: Participants performed an additional six blocks of trials in the curl force fields. Each block was composed of 160 curl field trials (20 for each of the 8 possible movements) and 42 generalization channel probe trials (one for each of the 21 different timing relations for both contexts). The phase totaled 1212 trials, with 960 trials conducted in the curl force fields and 252 within a channel.

Day2. The second session included a training phase in the curl force field to reinforce adaptation, followed by an extended generalization phase to measure the temporal generalization.

Training phase: Participants performed ten blocks of training trials. Each block comprised 16 curl field trials and 2 channel trials, totaling 180 trials for this phase.

Generalization phase: Participants were exposed to seven blocks. Each block consisted of 160 curl field trials and 42 generalization channel probe trials (1 for each of the 21 different timing relations for both contexts). For the analysis of the temporal generalization, only data from this phase was used. This phase totaled 1414 trials (1120 curl field trials and 294 generalization channel trials).

Experiments

Participants were randomly assigned to participate in one of three experiments. The experimental design for all three experiments was identical, except for the timing relation between the two hands during the training condition.

Experiment 1 – Past Context. In Experiment 1, participants first executed the contextual movement with their right-hand, followed by the adaptation movement with their left-hand. The onset of the adaptation movement was cued to start 750 ms after the onset of the contextual movement. We define this as a bimanual movement timing of -750 ms.

Experiment 2 – Simultaneous Context. In Experiment 2, participants moved both hands (contextual and adaptation movements) at the same time. This corresponds to a bimanual movement timing of 0ms.

Experiment 3 – Future Context. In Experiment 3, participants first executed the adaptation movement with their left-hand, followed by the right-hand contextual movement. The onset of the adaptation movement occurred 750 ms before the onset of the contextual movement, corresponding to a bimanual movement timing of +750 ms.

Data Analysis

The analysis was conducted offline using MATLAB R2023a. To examine learning and generalization, kinematic error and force compensation were calculated for each trial.

Kinematic Error. For each trial performed in null and viscous curl force fields, the kinematic error was determined from the adaptation phase of the movement. This was quantified by calculating the Maximum Perpendicular Error (MPE), defined as the maximum deviation of the hand's path from a straight line connecting the starting location of the movement to the center of the target. For each participant, an average MPE was computed over a set of sixteen trials. To correctly combine results from

Clockwise (CW) and Counterclockwise (CCW) field trials, the sign of the MPE was appropriately adjusted. Subsequently, the mean and standard error (SE) of the MPE were calculated across all participants.

Force Compensation. During each channel trial, the force exerted by the participants perpendicular to the wall of the simulated channel was measured. This measurement was used to estimate predictive feedforward adaptation, both during learning and in determining generalization to different temporal relations between the two hands. This method offers greater accuracy than relying solely on a reduction in kinematic error, as it avoids the effect of limb impedance due to muscle co-contraction [69–72]. Additionally, it provides an estimate of the adaptation throughout the entire movement, rather than at just a single time point. Force compensation is calculated by regressing the actual force measured on the channel wall against the force required to perfectly compensate for the force field (calculated as the movement velocity multiplied by the force field strength). This process yielded an estimate of the level of predictive force compensation for each channel trial [73].

To examine adaptation, the force compensation values for each participant were averaged over the two adjacent channel trials within each block of eighteen trials, representing the two different contexts. This approach ensured that the force compensation value reflected the degree of adaptation to both force fields. Subsequently, the mean and standard error (SE) of these force compensation values were calculated and analyzed across all participants throughout the duration of the experiment.

Bimanual Timing Relation. Channel probe trials were employed to examine the generalization of force compensation across 21 different timing relations between the limbs, spanning a ±1.8 second range. Although these timing relations were cued to participants to initiate specific movements, in practice, the participants often moved with timing relations slightly different from those requested. Therefore, to estimate the actual bimanual timing relations executed by participants, we calculated the start of each movement from each hand based on specific position and speed criteria. A hand was considered to have initiated movement when it deviated more than 2 mm from the starting target radius (1.27 cm from the center of the start) and was traveling at a speed greater than 5 cm/s. The bimanual temporal relation between the two arms for a given trial was calculated by subtracting the starting time of the left (adaptation) hand movement from the starting time of the right (contextual) hand movement. Therefore, negative values indicate that the contextual hand moved before the adaptation hand.

Temporal Generalization. To quantify the temporal generalization of the motor memory, we exclusively used the force compensation data measured during the channel trials from the Generalization Phase on the second day (refer to Fig. 1E). This specific data set was chosen because participants had achieved a higher level of adaptation to the curl field than they had during the first day. Importantly, we quantified temporal generalization as a function of the actual timing relations between the two hands. For each participant, compensation estimates from the

channel trials were first allocated to a series of temporal bins based on their bimanual timings. In total, 29 bins were utilized, with the center of each bin ranging from -2.1 to +2.1 seconds, and each bin was spaced by 150 ms intervals. The bins were selected so that their center timings (and widths) matched those used for cueing movements in the generalization probe channel trials.

For each bin, we calculated the mean and the number of bin counts for each participant. If, for any single participant, no compensation values were present in a bin, we removed that bin from our analysis. This precaution was taken to avoid generating potentially misleading overall estimates based on insufficient data points. To estimate generalization as a function of temporal relationships, we calculated the mean and standard error of the mean (SEM) for the bin values across all eight participants.

Statistics

Statistical analyses were performed in JASP 0.18.1 [74]. A Mauchly test was applied to check for sphericity wherever applicable. In the case that the Mauchly test was significant, the degrees of freedom were adjusted using a Greenhouse-Geisser correction. The α-level was set to .05 in all tests. We report omega squared as the effect size (ω^2).

For each experiment, we performed repeated measures ANOVAs to examine differences in the MPE and force compensation within each experiment. We compared the final pre-exposure MPE (mean of last block in pre-exposure), initial exposure MPE (mean of first block in exposure) and final exposure MPE (mean of final block on day2) using a repeated measures ANOVA with repeated factor of phase (3 levels). If a significant main effect was found, post-hoc comparisons were performed (Holm-Bonferroni corrected). For the force compensation, we compared the final pre-exposure (mean of last block in pre-exposure) and final exposure (mean of final block on day2) using a repeated measures ANOVA with a repeated factor of phase (2 levels: pre-exposure and final exposure).

To compare across experiments, we performed ANOVAs on the MPE and force compensation in the final exposure block with a factor of experiment condition (3 levels). If a significant main effect was found, post-hoc comparisons were performed (Holm-Bonferroni corrected).

To compare the temporal generalization within each experiment and across the three experiments we performed a repeated measures ANOVA with a repeated factor of timing (21 levels) and between subjects factor of experimental condition (3 levels). If a significant main effect was found, post-hoc comparisons were performed (Holm-Bonferroni corrected for the whole family of comparisons). Only post-hoc comparisons which were relevant for the study were examined and reported. Specifically, we only examined differences across timings within one experiment, or differences across experiments for each timing.

Author Contributions

The study was conceived and designed by ISH and DWF. The study was implemented by ISH. The experiments were conducted by SF. Data analysis was carried out by ISH. Figures were prepared by ISH and DWF. Statistics were performed by DWF. The manuscript was written by ISH, SF and DWF. The final manuscript was reviewed and edited by ISH, SF and DWF.

Competing Interest Statement

The authors declare that they have no financial, personal, or professional interests that could be construed to have influenced the paper.

Acknowledgements

Financial support was provided by the Technical University of Munich and the SECAM at the University of Plymouth.

References

1. Shadmehr, R. & Mussa-Ivaldi, F. A. Adaptive representation of dynamics during learning of a motor task. *J. Neurosci.* **14**, 3208–3224 (1994).
2. Lackner, J. R. & Dizio, P. Rapid adaptation to Coriolis force perturbations of arm trajectory. *J Neurophysiol* **72**, 299–313 (1994).
3. Kawato, M. Internal models for motor control and trajectory planning. *Current opinion in neurobiology* **9**, 718–727 (1999).
4. Shadmehr, R., Smith, M. A. & Krakauer, J. W. Error correction, sensory prediction, and adaptation in motor control. *Annual review of neuroscience* **33**, 89–108 (2010).
5. Conditt, M. A., Gandolfo, F. & Mussa-Ivaldi, F. A. The motor system does not learn the dynamics of the arm by rote memorization of past experience. *J Neurophysiol* **78**, 554–560 (1997).
6. Thoroughman, K. A. & Shadmehr, R. Learning of action through adaptive combination of motor primitives. *Nature* **407**, 742–747 (2000).
7. Donchin, O., Francis, J. T. & Shadmehr, R. Quantifying generalization from trial-by-trial behavior of adaptive systems that learn with basis functions: theory and experiments in human motor control. *J Neurosci* **23**, 9032–9045 (2003).
8. Orschiedt, J. & Franklin, D. W. Learning context shapes bimanual control strategy and generalization of novel dynamics. *PLoS Comput Biol* **19**, e1011189 (2023).
9. Howard, I. S. & Franklin, D. W. Neural Tuning Functions Underlie Both Generalization and Interference. *PloS one* **10**, e0131268 (2015).
10. Howard, I. S. & Franklin, D. W. Adaptive tuning functions arise from visual observation of past movement. *Sci Rep* **6**, 28416 (2016).

11. Sarwary, A. M. E., Stegeman, D. F., Selen, L. P. J. & Medendorp, W. P. Generalization and transfer of contextual cues in motor learning. *J Neurophysiol* **114**, 1565–1576 (2015).
12. Howard, I. S., Franklin, S. & Franklin, D. W. Asymmetry in kinematic generalization between visual and passive lead-in movements are consistent with a forward model in the sensorimotor system. *PLoS ONE* **15**, e0228083 (2020).
13. Shadmehr, R. & Brashers-Krug, T. Functional stages in the formation of human long-term motor memory. *J Neurosci* **17**, 409–419 (1997).
14. Karniel, A. & Mussa-Ivaldi, F. A. Does the motor control system use multiple models and context switching to cope with a variable environment? *Exp Brain Res* **143**, 520–524 (2002).
15. Osu, R., Hirai, S., Yoshioka, T. & Kawato, M. Random presentation enables subjects to adapt to two opposing forces on the hand. *Nature Neuroscience* **7**, 111–112 (2004).
16. Krakauer, J. W. & Shadmehr, R. Consolidation of motor memory. *Trends in neurosciences* **29**, 58–64 (2006).
17. Nozaki, D., Kurtzer, I. & Scott, S. H. Limited transfer of learning between unimanual and bimanual skills within the same limb. *Nature Neuroscience* **9**, 1364–1366 (2006).
18. Hirashima, M. & Nozaki, D. Distinct Motor Plans Form and Retrieve Distinct Motor Memories for Physically Identical Movements. *Current Biology* **22**, 432–436 (2012).
19. Howard, I. S., Ingram, J. N., Franklin, D. W. & Wolpert, D. M. Gone in 0.6 seconds: the encoding of motor memories depends on recent sensorimotor States. *J Neurosci* **32**, 12756–68 (2012).
20. Howard, I. S., Wolpert, D. M. & Franklin, D. W. The effect of contextual cues on the encoding of motor memories. *J Neurophysiol* **109**, 2632–44 (2013).
21. Forano, M., Schween, R., Taylor, J. A., Hegele, M. & Franklin, D. W. Direct and indirect cues can enable dual adaptation, but through different learning processes. *J Neurophysiol* **126**, 1490–1506 (2021).
22. Howard, I. S., Wolpert, D. M. & Franklin, D. W. The value of the follow-through derives from motor learning depending on future actions. *Curr Biol* **25**, 397–401 (2015).
23. Sheahan, H. R., Franklin, D. W. & Wolpert, D. M. Motor planning, not execution, separates motor memories. *Neuron* **92**, 773–9 (2016).
24. Howard, I. S., Ingram, J. N. & Wolpert, D. M. Context-dependent partitioning of motor learning in bimanual movements. *J Neurophysiol* **104**, 2082–2091 (2010).
25. Gippert, M. *et al.* Prior Movement of One Arm Facilitates Motor Adaptation in the Other. *J. Neurosci.* **43**, 4341–4351 (2023).
26. Yokoi, A., Hirashima, M. & Nozaki, D. Gain Field Encoding of the Kinematics of Both Arms in the Internal Model Enables Flexible Bimanual Action. *J Neurosci* **31**, 17058–17068 (2011).
27. Franklin, S., Leib, R., Dimitriou, M. & Franklin, D. W. Congruent visual cues speed dynamic motor adaptation. *J Neurophysiol* **130**, 319–331 (2023).
28. Gonzalez Castro, L. N., Monsen, C. B. & Smith, M. A. The binding of learning to action in motor adaptation. *PLoS Comput Biol* **7**, e1002052 (2011).

29. Joiner, W. M., Ajayi, O., Sing, G. C. & Smith, M. A. Linear hypergeneralization of learned dynamics across movement speeds reveals anisotropic, gain-encoding primitives for motor adaptation. *J Neurophysiol* **105**, 45–59 (2011).
30. Berniker, M., Franklin, D. W., Flanagan, J. R., Wolpert, D. M. & Kording, K. Motor learning of novel dynamics is not represented in a single global coordinate system: evaluation of mixed coordinate representations and local learning. *J Neurophysiol* **111**, 1165–1182 (2014).
31. Leib, R. & Franklin, D. W. Error Prediction Determines the Coordinate System Used for Novel Dynamics Representation. *bioRxiv* (2021) doi:https://doi.org/10.1101/2021.01.04.425325.
32. Poggio, T. & Bizzi, E. Generalization in vision and motor control. *Nature* **431**, 768–774 (2004).
33. Kadiallah, A., Franklin, D. W. & Burdet, E. Generalization in adaptation to stable and unstable dynamics. *PloS one* **7**, e45075 (2012).
34. Shadmehr, R. Generalization as a behavioral window to the neural mechanisms of learning internal models. *Human Movement Science* **23**, 543–568 (2004).
35. Howard, I. S., Ingram, J. N., Körding, K. P. & Wolpert, D. M. Statistics of natural movements are reflected in motor errors. *J Neurophysiol* **102**, 1902–1910 (2009).
36. Kelso, J. A. S. *Dynamic patterns: the self-organization of brain and behavior*. (MIT Press, 1995).
37. Kobayashi, T. & Nozaki, D. Motor control and adaptation in a redundant motor task manipulating a stick with both hands. *bioRxiv* (2023) doi:https://doi.org/10.1101/2023.06.13.544873.
38. Howard, I. S., Ford, C., Cangelosi, A. & Franklin, D. W. Active lead-in variability affects motor memory formation and slows motor learning. *Sci Rep* **7**, 7806 (2017).
39. Swinnen, S. P. Intermanual coordination: From behavioural principles to neural-network interactions. *Nat Rev Neurosci* **3**, 348–359 (2002).
40. Gerloff, C. & Andres, F. G. Bimanual coordination and interhemispheric interaction. *Acta Psychologica* **110**, 161–186 (2002).
41. Cross, K. P., Heming, E. A., Cook, D. J. & Scott, S. H. Maintained Representations of the Ipsilateral and Contralateral Limbs during Bimanual Control in Primary Motor Cortex. *J. Neurosci.* **40**, 6732–6747 (2020).
42. Donchin, O., Gribova, A., Steinberg, O., Bergman, H. & Vaadia, E. Primary motor cortex is involved in bimanual coordination. *Nature* **395**, 274–278 (1998).
43. Steinberg, O. *et al.* Neuronal populations in primary motor cortex encode bimanual arm movements. *Eur J of Neuroscience* **15**, 1371–1380 (2002).
44. Wolpert, D. M., Miall, R. C. & Kawato, M. Internal models in the cerebellum. *Trends in Cognitive Sciences* **2**, 338–347 (1998).
45. Imamizu, H. *et al.* Human cerebellar activity reflecting an acquired internal model of a new tool. *Nature* **403**, 192–195 (2000).
46. Ito, M. Bases and implications of learning in the cerebellum — adaptive control and internal model mechanism. *Progress in Brain Research* **148**, 95–109 (2005).
47. Scott, S. H. The computational and neural basis of voluntary motor control and planning. *Trends in cognitive sciences* **16**, 541–549 (2012).

48. Franklin, D. W., Reichenbach, A., Franklin, S. & Diedrichsen, J. Temporal Evolution of Spatial Computations for Visuomotor Control. *J Neurosci* **36**, 2329–2341 (2016).
49. Makino, H., Hwang, E. J., Hedrick, N. G. & Komiyama, T. Circuit Mechanisms of Sensorimotor Learning. *Neuron* **92**, 705–721 (2016).
50. Česonis, J. & Franklin, D. W. Contextual cues are not unique for motor learning: Task-dependant switching of feedback controllers. *PLoS Comput Biol* **18**, e1010192 (2022).
51. Leib, R., Howard, I. S., Millard, M. & Franklin, D. W. Behavioral Motor Performance. *Comprehensive Physiology* 5179–5224 (2024) doi:https://doi.org/10.1002/cphy.c220032.
52. Klapp, S. T. Doing two things at once: The role of temporal compatibility. *Memory & Cognition* **7**, 375–381 (1979).
53. Swinnen, S. P. & Wenderoth, N. Two hands, one brain: cognitive neuroscience of bimanual skill. *Trends in Cognitive Sciences* **8**, 18–25 (2004).
54. Desmurget, M. & Grafton, S. Forward modeling allows feedback control for fast reaching movements. *Trends in cognitive sciences* **4**, 423–431 (2000).
55. Wolpert, D. M. & Flanagan, J. R. Motor prediction. *Curr Biol* **11**, R729-32 (2001).
56. Flanagan, J. R., Vetter, P., Johansson, R. S. & Wolpert, D. M. Prediction precedes control in motor learning. *Curr Biol* **13**, 146–150 (2003).
57. Franklin, D. W. & Wolpert, D. M. Computational mechanisms of sensorimotor control. *Neuron* **72**, 425–442 (2011).
58. Chow, J. *et al.* Comparing the pre- and post-impact ball and racquet kinematics of elite tennis players' first and second serves: a preliminary study. *Journal of Sports Sciences* **21**, 529–537 (2003).
59. Cisek, P. Evolution of behavioural control from chordates to primates. *Phil. Trans. R. Soc. B* **377**, 20200522 (2022).
60. Cisek, P. & Hayden, B. Y. Neuroscience needs evolution. *Phil. Trans. R. Soc. B* **377**, 20200518 (2022).
61. Lee, J.-Y. & Schweighofer, N. Dual adaptation supports a parallel architecture of motor memory. *J Neurosci* **29**, 10396–10404 (2009).
62. Forano, M. & Franklin, D. W. Timescales of motor memory formation in dual-adaptation. *PLoS Comput Biol* **16**, e1008373 (2020).
63. Heald, J. B., Lengyel, M. & Wolpert, D. M. Contextual inference underlies the learning of sensorimotor repertoires. *Nature* **600**, 489–493 (2021).
64. Heald, J. B., Lengyel, M. & Wolpert, D. M. Contextual inference in learning and memory. *Trends in Cognitive Sciences* **27**, 43–64 (2023).
65. Oldfield, R. C. The assessment and analysis of handedness: the Edinburgh inventory. *Neuropsychologia* **9**, 97–113 (1971).
66. Howard, I. S., Ingram, J. N. & Wolpert, D. M. A modular planar robotic manipulandum with end-point torque control. *J Neurosci Meth* **181**, 199–211 (2009).
67. Gandolfo, F., Mussa-Ivaldi, F. A. & Bizzi, E. Motor learning by field approximation. *PNAS* **93**, 3843–3846 (1996).
68. Scheidt, R. A., Reinkensmeyer, D. J., Conditt, M. A., Rymer, W. Z. & Mussa-Ivaldi, F. A. Persistence of motor adaptation during constrained, multi-joint, arm movements. *J Neurophysiol* **84**, 853–862 (2000).

69. Milner, T. E. & Franklin, D. W. Impedance control and internal model use during the initial stage of adaptation to novel dynamics in humans. *J Physiol* **567**, 651–664 (2005).
70. Franklin, D. W., Burdet, E., Osu, R., Kawato, M. & Milner, T. E. Functional significance of stiffness in adaptation of multijoint arm movements to stable and unstable dynamics. *Exp Brain Res* **151**, 145–157 (2003).
71. Franklin, S. & Franklin, D. W. Feedback Gains modulate with Motor Memory Uncertainty. *Neurons, Behavior, Data analysis, and Theory* **5**, (2021).
72. Franklin, S. & Franklin, D. W. Visuomotor feedback tuning in the absence of visual error information. *Neurons, Behavior, Data analysis, and Theory* (2023) doi:10.51628/001c.91252.
73. Smith, M. A., Ghazizadeh, A. & Shadmehr, R. Interacting adaptive processes with different timescales underlie short-term motor learning. *PLoS Biology* **4**, e179 (2006).
74. JASP Team. JASP (Version 0.18.1) [Computer Software]. (2023).